Structure and Dynamic Behavior of (η^3-Allyl)bromodicarbonylmolybdenum(II) Complexes Containing Polydentate 2-Pyridylphosphanes or Their Oxides as Chelating Ligands: Occurrence of Three Fluxional Processes

Pablo Espinet,*[a] Rosa Hernando,[a] Gonzalo Iturbe,[a] Fernando Villafañe,[a] A. Guy Orpen,[b] and Isabel Pascual[b]

Keywords: Molybdenum / Fluxionality / Pyridylphosphanes / Phosphane oxides / Polydentate ligands

The pseudo-octahedral complexes [Mo(η^3-allyl)Br(CO)$_2$(P-Py$_n$Ph$_{3-n}$-*P,N*)] (Py = 2-pyridyl; n = 2, 3) and [Mo(η^3-allyl)Br(CO)$_2$(OPPy$_m$Ph$_{3-m}$-*O,N*)] (m = 1, 2, 3) undergo three different dynamic processes in solution, depending on the chelating ligand. The complexes containing PPhPy$_2$ and PPy$_3$ as chelating *P,N*-donors undergo a novel "pivoted double switch" mechanism which scrambles two *equatorial* coordination sites with racemization, while maintaining the identity of the phosphorus atom *trans* to the allyl ligand. The complexes containing 2-pyridylphosphane oxides as chelating *O,N*-donors undergo a nondissociative intramolecular trigonal-twist (or turnstile) rearrangement which maintains the identity of the phosphane oxide oxygen atom coordinated in an *equatorial* position. All the complexes containing uncoordinated pyridyls undergo a slow dissociative exchange of pyridyls without coordination site scrambling. The structure of the complex [Mo(η^3-allyl)Br(CO)$_2$(OPPy$_3$-*O,N*)] has been determined by X-ray diffraction.

Introduction

The coordination of 2-pyridylphosphanes or their P-substituted derivatives has allowed the elucidation of many dynamic processes in solution. Our group is currently carrying out a study of their behavior with different metals, such as palladium, platinum[1] and molybdenum.[2] In the course of these studies, we decided to explore the behavior of 2-pyridylphosphanes[3] or their oxides towards (η^3-allyl)bromodicarbonylmolybdenum(II), with the aim of understanding how the ligands coordinate to this metal moiety (there are very few reports on hybrid chelating or tripodal ligands coordinated to this system), and examine possible dynamic processes in solution.

The complexes [Mo(η^3-allyl)X(CO)$_2$(L^1)(L^2)] (X = anionic ligand; L^1, L^2 = two monodentate neutral ligands, or one bidentate neutral ligand), show two possible solid state structures, as depicted in Figure 1 (**A** and **B**). Both are pseudo-octahedral complexes if the η^3-allyl ligand is considered as occupying one coordination site with its terminal atoms oriented over the carbonyl groups, which has been demonstrated to be the most energetically favorable arrangement.[4] In structure **A** the anionic ligand occupies the *axial* position, *trans* to the allyl group, giving rise to C_s symmetry with a σ plane which bisects the allyl group and contains the metal atom, whereas in structure **B** the anionic ligand X occupies one of the *equatorial* positions leading to a C_1 geometry. The adoption of one of these two possible arrangements in the solid state does not seem to follow clear rules. Structure A is usually observed when X is a halogen or a pseudohalogen and L–L is a bidentate nitrogen donor ligand, such as bipy.[5] However, structure B has been found for trifluoroacetate as the anionic ligand and 1,10-phenanthroline as the chelate,[6] or when the neutral ligands are two pyrazols and bromide is the anionic ligand.[7]

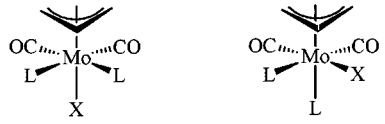

Figure 1. Two possible structures, **A** and **B**, for [Mo(η^3-allyl)X(CO)$_2$(L^1)(L^2)]

Several solution dynamic processes have been detected for this type of complex: the nondissociative trigonal-twist rearrangement[8] or turnstile mechanism,[1c,9] in which there is an intramolecular rotation of the "XL$_2$" face, was first established for L$_2$ = diphosphane and X = halogen. This process has since then been observed for a variety of "XL$_2$" systems, including cationic complexes with XL$_2$ = neutral tridentate nitrogen donor ligand.[10] Other solution processes detected for these complexes are the substitution of the neutral ligands (usually nitrogen donors) by solvents such as MeCN or water,[10b,11] and the η^3–η^1–η^3 rearrangement of the allyl ligand, which has been proposed for tridentate nitrogen donor ligands such as trispyrazolylborate or bispyrazolylaminomethane.[12]

[a] Departamento de Química Inorgánica, Facultad de Ciencias, Universidad de Valladolid, 47005 Valladolid, Spain
E-mail: espinet@qi.uva.es
[b] School of Chemistry, University of Bristol, Bristol BS8 1TS, U.K.
E-mail: Guy.Orpen@bris.ac.uk
Supporting Information for this article is available on the WWW under http://www.wiley-vch.de/home/eurjic or from the author.

  1434–1948/00/0505–1031 $ 17.50+.50/0

Results and Discussion

[Mo(η³-allyl)Br(CO)$_2$(PPy$_n$Ph$_{3-n}$-*P,N*)] (*n* = 2, 3)

The complexes [Mo(η³-allyl)Br(CO)$_2$(PPy$_n$Ph$_{3-n}$-*P,N*)] [*n* = 2 (**1**), 3 (**2**)] were obtained by displacement of the nitrile ligands in [Mo(η³-allyl)Br(CO)$_2$(MeCN)$_2$] with PPy$_2$Ph or PPy$_3$.[13] All attempts to obtain a similar complex with PPyPh$_2$ were unsuccessful. This may be due to electronic factors since PPyPh$_2$ is a weaker donor than the other pyridylphosphanes.[14] The IR spectra of **1** and **2** in the C–O stretching region show two bands, as expected for *cis* dicarbonyl complexes. Their low electrical conductivity in solution indicates that the complexes are neutral, supporting coordination of the bromo ligand to the molybdenum atom.

Characterization of [Mo(η³-allyl)Br(CO)$_2$(PPy$_2$Ph-*P,N*)] (1)

The low temperature ^{1}H NMR spectrum (–60 °C) corresponds to an asymmetric complex, the signals of the allyl group displaying the expected ABCDX pattern. Two doublets are observed for the H^6 protons of the pyridyls: one at very low field (9.60 ppm) typical of a pyridyl ligand coordinated *cis* to a halogen ligand, as has been clearly established for square planar geometries;[15] and the second (9.12 ppm) in the typical range of H^6 for uncoordinated pyridyls. Thus, for complex **1** at low temperature, these data support the *P,N*-coordination of the PPy$_2$Ph ligand.

However, a symmetrically averaged spectrum (revealing a racemization process) is observed at high temperature (+55 °C): the allyl group displays an A$_2$M$_2$X pattern where both H^{anti} are equivalent, as well as both H^{syn}, and only one doublet (9.46 ppm) is detected for both pyridyl H^6 atoms. Therefore, the dynamic process detected results in simultaneous equivalence of the two pyridyl groups and both ends of the allyl group. The phosphorus atom of PPy$_2$Ph is not directly involved in the dynamic process, and its chemical shift remains practically unchanged from –60 °C to +55 °C (–8.7 ppm in the ^{31}P{^{1}H} NMR spectra). This implies it coordinates in the *axial* position *trans* to the allyl group in a structure of type B (Figure 1).

The only process consistent with this NMR behavior is the racemization shown in Scheme 1 (R = Ph for **1**). In this exchange process, the pyridyl groups always occupy the same position when coordinated, and the Br ligand switches between two *equatorial* positions. We will refer to this process as a "pivoted double switch" mechanism.

Both the geometry of the molecule and the dynamic process in complex **1** were confirmed by a phase sensitive 2-D ^{1}H NOESY spectrum recorded at –50 °C, shown in Figure 2. At this temperature, the significant signals have split and the interchange process is slow. In Figure 2 a (positive peaks), cross-peaks due to chemical exchange of magnetization are detected between both H^{syn}, and also between both H^{anti} of the allyl group (the latter are difficult to observe because their signals almost overlap); whereas for the aromatic protons, cross-peaks relate the H^6 protons of the coordinated and uncoordinated pyridyls at this temperature. Figure 2b shows negative cross peaks due to NOEs between both H^6–H^{central}, H^{syn}–H^{anti}, and H^6–other aromatic protons. The latter two are expected NOEs, and do not provide structural information, but the first correlation indicates a close spatial proximity of the H^{central} of the allyl ligand and both H^6 atoms. A similar NOE has been reported for a complex containing a phenanthroline coordinated in the

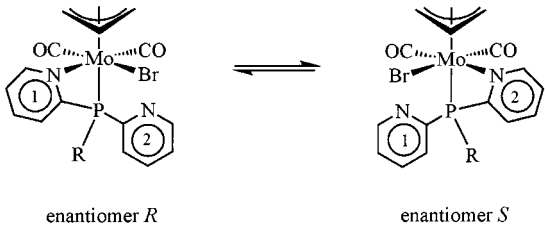

Scheme 1. "Pivoted double switch" mechanism in complexes **1** (R = Ph) and **2** (R = Py)

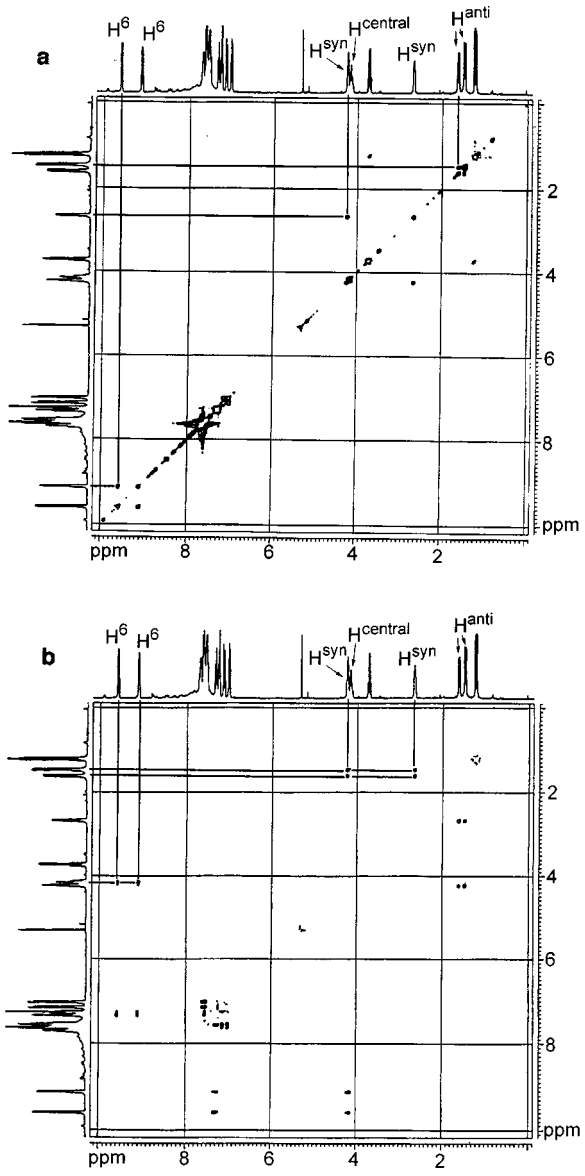

Figure 2. Phase sensitive 2-D NOESY experiment carried out for **1** at –50 °C. (a) Positive peaks due to chemical exchange of magnetization. (b) Negative peaks due to NOEs

same position as the pyridyl in our system.[6] The observation of two intense cross-peaks between $H^{central}$ and the two H^6 at lower field in complex **1** must presumably be related to the dynamic process shown in Scheme 1.

Characterization of [Mo(η^3-allyl)Br(CO)$_2$(PPy$_3$-*P,N*)] (2)

All the main features observed for **1** are also detected for **2**. The $^{31}P\{^1H\}$ NMR spectra at different temperatures (from +55 °C to –60 °C) show only one invariant singlet at –10.0 ppm. The ^1H NMR spectrum at –60 °C supports the existence of only one asymmetric complex in solution (which is a racemic mixture, as before), where three doublets are observed for the H^6 protons of the three pyridyls present: one at very low field (9.56 ppm) for the pyridyl coordinated *cis* to the bromo ligand,[15] and two more for the H^6 of the uncoordinated pyridyls (9.11 and 8.98 ppm). The ^1H NMR spectra at room temperature and above correspond to a symmetric averaged species where the allyl group displays the expected A_2M_2X pattern, and the signals of two H^6 (one coordinated and one uncoordinated) have coalesced to one broad signal, whereas the H^6 of the third pyridyl (that at higher field) remains nonequivalent. This indicates that the exchange process depicted in Scheme 1 (with R = Py in **2**) affects only one of the two uncoordinated pyridyls, the one which is able to coordinate by virtue of its geometry.

The ^1H NMR spectrum at 55 °C shows a slight broadening of all the signals, which is not observed in the spectrum of **1** at this temperature, suggesting that the third pyridyl begins to become involved in a second, and slower, exchange process. This second process interchanging the third pyridyl with the other two is too slow to be detected by variable temperature NMR (decomposition of the sample is observed upon further heating), but could be confirmed by a phase sensitive 2-D ^1H NOESY experiment. Chemical exchange is detected between both H^{syn}, between both H^{anti}, and between two H^6 (as for **1**), but in addition less intense cross peaks relating these two H^6 with the third H^6 (8.98 ppm) are also observed, supporting the involvement of the third pyridyl (R in Scheme 1) in a slower exchange equilibrium.

Discussion of the Dynamic Process of Complexes 1 and 2

The dynamic process shown in Scheme 1 for complexes **1** and **2** seems not to have precedent in the literature for the (η^3-allyl)bromodicarbonylmolybdenum(II) system, so the mechanism of interconversion deserves further discussion. All dissociative mechanisms can be discarded. An η^3–η^1–η^3 rearrangement of the allyl ligand would render H^{anti} and H^{syn} equivalent giving an A_4X pattern for the allyl group in the ^1H NMR spectra, which is not observed. A mechanism involving dissociation of the coordinated pyridyl ligand with concomitant rotation about the Mo–P may also be discounted, as the second slow process detected for **2**, which exchanges the three pyridyls, in fact requires decoordination of the pyridyl to allow for rotation around the Mo–P bond and hence coordination of the third pyridyl (Scheme 1). Hence, if decoordination of the coordinated pyridyl was occurring for the process in Scheme 1, the exchange of the third pyridyl should take place at the same rate (assuming rotation about the Mo–P bond is rapid), which is not observed. Dissociation of the bromo ligand may also be discounted since addition of excess bromide [5:1 as NBu_4Br in $(CD_3)_2CO$ solution of **2**][16] did not reduce the exchange rate.

To ascertain whether the dynamic process was associative, $\Delta S^{\ddagger}$ was determined by line shape analysis using the DNMR6 program for complex **2** (data taken from –40 to +40 °C). The value obtained, -2 ± 4 J mol^{-1} K^{-1}, is too low to unequivocally support an associative mechanism for this process, although values close to zero have been found for processes which have been finally identified as associative.[1b] Therefore, either an associative or a concerted mechanism may be proposed for this dynamic process, as the dissociative path can be definitely discarded.

[Mo(η^3-allyl)Br(CO)$_2$(OPPy$_n$Ph$_{3-n}$-*O,N*)] (*n* = 1, 2, 3)

The complexes [Mo(η^3-allyl)Br(CO)$_2$(OPPy$_n$Ph$_{3-n}$-*O,N*)] [*n* = 1 (**3**), 2 (**4**), 3 (**5**)] were obtained by displacement of the nitrile ligands in [Mo(η^3-allyl)Br(CO)$_2$(MeCN)$_2$] with the ligands $OPPyPh_2$, $OPPy_2Ph$, and $OPPy_3$ to obtain **3**, **4**, and **5**, respectively. Complex **4** could also be obtained by oxidative addition of allyl bromide to [Mo(CO)$_3$(OPPy$_2$Ph-*O,N*$_2$)].

The three complexes show two C–O stretching bands in the solid state, as expected for *cis* dicarbonyl complexes. Complexes **3** and **5** also display two C–O stretching bands in solution, whereas **4** shows four. According to the isomer equilibria discussed below, four bands should be expected (at least when all the isomers are noticeably abundant). However, the bands for each pair of isomers **C** and **D** are almost coincident (Figure 3). In fact careful examination of the IR C–O bands reveals that they are asymmetric and show shoulders, but the presence of **C** and **D** isomers only becomes clear in the NMR spectra. The IR spectra of the solid complexes **3–5** do not show bands in the 1300–1200 cm^{-1} region, where the P–O stretching absorptions of the free ligands are found. This implies coordination of the ligands as oxygen donors, although the assignment of the band due to P–O stretching is very difficult, due to the pres-

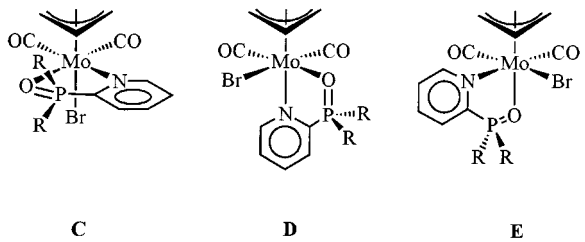

C **D** **E**

Figure 3. Three possible isomers C, D, and E, for complexes **3–5**

ence of other absorptions in the expected range for O-bonded phosphane oxides.[17]

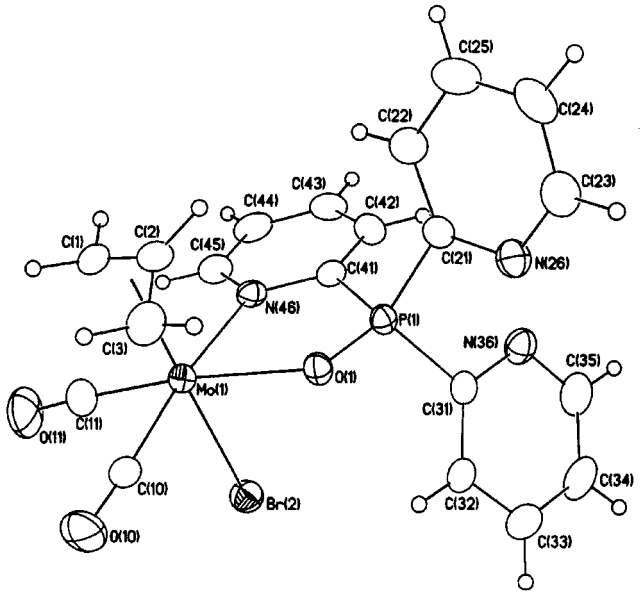

Figure 4. Displacement ellipsoid drawing of **5** showing the atom numbering scheme;tThe ellipsoids are drawn at 30% probability level

Table 1. Selected bond (Å) and angles (deg) for **5**

Mo(1)–C(10)	1.934(7)	Mo(1)–C(11)	1.934(8)
Mo(1)–C(1)	2.314(6)	Mo(1)–C(3)	2.301(7)
Mo(1)–C(2)	2.196(6)	Mo(1)–Br(2)	2.6429(8)
Mo(1)–O(1)	2.256(4)	Mo(1)–N(46)	2.323(5)
C(1)–C(2)	1.380(9)	C(2)–C(3)	1.415(9)
P(1)–O(1)	1.501(4)	P(1)–C(41)	1.817(6)
C(10)–O(10)	1.149(8)	C(11)–O(11)	1.130(8)
C(10)–Mo(1)–C(11)	78.7(3)	O(1)–Mo(1)–N(46)	76.8(2)
C(11)–Mo(1)–N(46)	99.5(3)	C(10)–Mo(1)–O(1)	103.5(2)
C(10)–Mo(1)–N(46)	171.0(2)	C(11)–Mo(1)–O(1)	170.0(2)
C(10)–Mo(1)–Br(2)	89.2(2)	C(11)–Mo(1)–Br(2)	85.5(2)
O(1)–Mo(1)–Br(2)	84.76(10)	N(46)–Mo(1)–Br(2)	81.87(11)
Mo(1)–N(46)–C(41)	120.8(4)	N(46)–C(41)–P(1)	113.4(4)
C(41)–P(1)–O(1)	108.8(3)	P(1)–O(1)–Mo(1)	120.1(2)
Mo(1)–C(1)–C(2)	67.7(3)	Mo(1)–C(3)–C(2)	67.7(4)
C(1)–C(2)–Mo(1)	76.9(4)	C(3)–C(2)–Mo(1)	75.7(4)
C(1)–C(2)–C(3)	115.1(6)		

The low electrical conductivities in solution indicate that the complexes **3–5** are neutral, with the bromo ligand coordinated to the molybdenum atom. Only the three isomers **C**, **D**, and **E**, shown in Figure 3, can be proposed in accordance with the IR and conductivity data. The molecules are chiral, and Figure 3 shows the *R* enantiomers only.

The $^{31}P\{^{1}H\}$ NMR spectra of complexes **3** and **5** show two singlets of different intensity at low temperature, which coalesce on heating. This implies that a dynamic process interchanging two of the three possible isomers in Figure 3 is occurring. Twice as many signals are observed in the $^{31}P\{^{1}H\}$ NMR spectra of **4**, that is, four singlets at –60 °C which coalesce to two singlets of different intensity at 50 °C. In this complex the R groups are different (Ph and Py), thus the isomers, which are enantiomers in **3** and **5** (and which therefore have indistinguishable NMR spectra) become diastereoisomers for **4**, doubling the number of signals; but again only two of the three structures **C**, **D**, or **E** are involved. The exchange process observed corresponds exactly to the trigonal-twist mechanism described in the literature for the complex [Mo(η³-allyl)I(CO)$_2$(arphos)],[8] and needs no further discussion except for identification of the two isomers involved. This was achieved as described below.

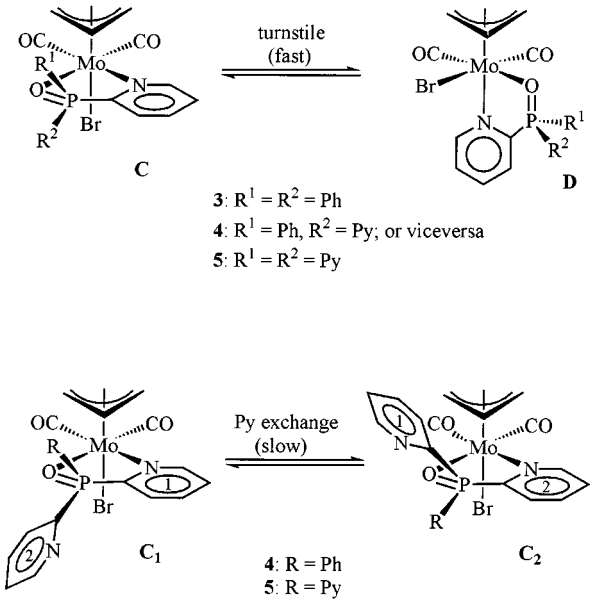

Scheme 2. Dynamic processes in complexes **3**, **4**, and **5**: fast nondissociative intramolecular trigonal-twist (or turnstile) rearrangement in complexes **3**, **4**, and **5** and slow pyridyl-exchange equilibria in complexes **4** and **5**

Structure of [Mo(η³-allyl)Br(CO)$_2$(OPPy$_3$-*O,N*)] (5)

An X-ray structural determination was carried out for [Mo(η³-allyl)Br(CO)$_2$(OPPy$_3$-*O,N*)] (**5**). The structure is shown in Figure 4, and Table 1 lists relevant distances and angles. The molybdenum atom is *pseudo*-octahedrally coordinated, assuming that the allyl group occupies one site. The two carbonyls and the allyl are mutually *cis*, with the terminal carbon atoms of the allyl moiety oriented over the carbonyls, as usually found for this class of complex.[4] The observed structure is of the form labeled **C** in Figure 3. The P–O distance is slightly elongated compared to those found in palladium(II) complexes containing the OPPy$_2$Ph ligand, where the oxygen atom is not coordinated to the metal: P–O = 1.480(2) and 1.482(2) Å in [Pd(C$_6$F$_5$)X(OPPy$_2$Ph-*N$_2$*)] (X = Br and C$_6$F$_5$, respectively)[1b] *cf.* 1.501(4) Å in **5**. The donor atoms of the OPPy$_3$ ligand coordinated in the *equatorial* positions have different donor properties, but this seems to induce very little asymmetry in the *trans* carbonyl groups: the Mo–C distances are equal [1.934(7) and 1.934(8) Å] and the C–O distances show insignificant differences [1.149(8) and 1.130(8) Å]. The allyl group is also essentially symmetrical [C–C = 1.380(9) and 1.415(9) Å; Mo–C^{terminal} = 2.314(6) and 2.301(7) Å]. This indicates that the different donor properties of the atoms in the *equatorial* sites do not induce observable asymmetry in the allyl ligand, as has been previously reported.[10a] The distances

and angles of the allyl group found in **5** are very similar to those reported for [Mo(η^3-allyl)(acac)$(CO)_2$(py)],[18] which also contains an oxygen donor ligand and a nitrogen donor ligand in the *equatorial* positions.

Discussion of the Dynamic Process of Complexes 3–5

When an NMR sample of **5** in $CDCl_3$ was prepared in a liquid nitrogen bath, and then allowed to melt and simultaneously dissolve at –60 °C in the NMR probe, only one isomer was found, which is logically assigned to structure **C**. The solution was then warmed to room temperature to establish the equilibrium between the isomers, and a phase sensitive 2-D ^{1}H NOESY spectrum was recorded at –50 °C. Negative peaks associated to NOE are not observed, which disfavors structure **E** for which an NOE between the coordinated pyridyl and some of the allyl protons would be expected (H^6–$H^{central}$ correlations were observed for **1** and **2**). Consequently, we assign structure **D** to the second isomer. Positive peaks were observed between $H^{central}$, and each H^{syn} and H^{anti} of the two isomers **C** and **D**, but not between the two H^{syn} or between the two H^{anti} atoms of each isomer. In other words, there was no racemization of the molecule and the two halves of the allyl group remained inequivalent during the fluxional processes. Finally, there were also weak cross peaks showing exchange of the coordinated and the free pyridyl groups.

Thus two types of exchange are operative in these systems, which are depicted in the general Scheme 2. The faster movement is a nondissociative intramolecular trigonal-twist (or turnstile) rearrangement, converting diastereoisomers **C** and **D**. This is the only mechanism operating for $R^1 = R^2 =$ Ph (in **3**). The second and slower movement (it is barely observed in the one dimensional spectrum of **5** at 55 °C as a broadening of the signals) is an exchange of pyridyls without racemization. In this respect, it is very different from the "pivoted double switch" as seen in **1** and **2**. The conservation of the asymmetry allows decoordination of the oxygen to give a *N,N*-bonded intermediate to be discounted, as this would create a symmetry plane. In fact, in conjunction with the observation of pyridyl exchange of **1** and **2**, a dissociative mechanism is more plausible, with the incoming pyridyl group taking the site left vacant by dissociation. This, as shown in Scheme 2, converts $\mathbf{C_1}$ to $\mathbf{C_2}$, these being identical for **5**, but diastereoisomers for **4**. The slowness of this mechanism is also consistent with a dissociative process.

Conclusion

The systems studied here reveal the existence of three mechanisms, depending on the chelating ligand. The slowest mechanism is common to both ligands that have uncoordinated pyridyls, which is a dissociative exchange of pyridyls without scrambling of coordination sites. The second, shown by the pyridylphosphane oxides, is the well-known nondissociative intramolecular trigonal-twist (or turnstile) mechanism, which produces scrambling of the coordination sites but retaining the elements of chirality (i.e. without racemization). Finally, for bis- or trispyridylphosphane, the pendant pyridyl triggers a novel "pivoted double switch" mechanism scrambling two coordination sites with racemization. A different but somewhat related case has been discussed in detail elsewhere.[19]

Experimental Section

General Remarks: All reactions were carried out under an atmosphere of pre-purified dinitrogen. Solvents were purified according to standard procedures.[20] [Mo(η^3-allyl)Br$(CO)_2$(MeCN)$_2$],[21] [Mo$(CO)_3$($OPPy_2$Ph-*O,N*$_2$)],[2b] and 2-pyridylphosphanes were prepared as previously described,[22] and their oxides were synthesized by standard methods.[23] The synthesis of [Mo(η^3-allyl)Br$(CO)_2$(P-Py_2Ph-*P,N*)] has been previously reported.[2a]

The progress of the reactions involving carbonyl complexes was monitored by solution IR spectra in the 2100–1700 cm^{-1} region. Filtrations were carried out on dry Celite without exclusion of air. The products are air-stable solids which were recrystallized at –20 °C.

Infrared spectra were recorded on Perkin–Elmer 883 or 1720X apparatus in NaCl cells for solutions, and as Nujol mulls or KBr pellets for solids. NMR spectra were recorded on Bruker AC-300 or ARX-300 instruments in $CDCl_3$. NMR spectra were referred to TMS or 85% aqueous H_3PO_4. Elemental analyses were performed on a Perkin–Elmer 2400B microanalyzer. The electrical conductivity measurements were carried out at room temperature with a Crison 522 conductivity meter using $5 \cdot 10^{-4}$ M solutions; the range of molar conductivity for 1:1 electrolytes is 75–95 $S \cdot cm^2 \cdot mol^{-1}$ in nitromethane solutions.[24]

General Method for the Preparation of the Complexes: A 100 mL Schlenk flask was successively charged with equimolar amounts (0.2–0.5 mmol) of [Mo(η^3-allyl)Br$(CO)_2$(MeCN)$_2$], the respective ligand, and CH_2Cl_2 (10–25 mL). The solution was stirred at room temperature for 15 min., and then EtOH or hexane was added (5–15 mL). Concentration of the solution in vacuo and cooling to –20 °C gave microcrystalline solids, which were filtered, washed with Et_2O (3 × 3 mL approximately), and dried in vacuo. The yields, color, and spectroscopic data of the products obtained are given below.

[Mo(η^3-allyl)Br$(CO)_2$(PPy_2Ph-*P,N*)] (1):[2a] $^{31}P\{^1H\}$ NMR (room temp.): δ = –8.7 (s). – ^{1}H NMR (55 °C): δ = 9.46 (d, *J* = 5 Hz, 2 H^6 of coordinated + uncoordinated Py), 7.76 (m, 3 H), 7.63 (m, 2 H), 7.52 (m, 2 H), 7.27 (m, 2 H), 7.07 (d, *J* = 8 Hz, 2 H), 4.15 (m, 1 H^c), 3.40 (br, 2 H^s), 1.54 (d, *J* = 9.5 Hz, 2 H^a). – ^{1}H NMR (room temp.): δ = 9.43 (br, 2 H^6 of coordinated + uncoordinated Py), 7.72 (m, 3 H), 7.63 (m, 2 H), 7.53 (m, 2 H), 7.28 (m, 2 H), 7.08 (d, *J* = 8 Hz, 2 H), 4.15 (m, 1 H^c), 1.54 (d, *J* = 9.5 Hz, 2 H^a). – ^{1}H NMR (–60 °C): δ = 9.60 (d, *J* = 5.5 Hz, 1 H^6 of coordinated Py), 9.12 (d, *J* = 5.5 Hz, 1 H^6 of uncoordinated Py), 7.63 (m, 7 H), 7.34 (t, *J* = 6 Hz, 1 H), 7.27 (t, *J* = 6 Hz, 1 H), 7.16 (d, *J* = 8 Hz, 1 H), 7.03 (d, *J* = 8 Hz, 1 H), 4.24 (br, 1 H^s), 4.17 (m, 1 H^c), 2.67 (br, 1 H^s), 1.63 (d, *J* = 10 Hz, 1 H^a), 1.48 (d, *J* = 10 Hz, 1 H^a). Other spectroscopic and analytical data have been reported previously.[2a]

[Mo(η^3-allyl)Br$(CO)_2$(PPy_3-*P,N*)] (2): 46%, yellow. – $^{31}P\{^1H\}$ NMR (room temp.): δ = –10.0 (s). – ^{1}H NMR (55 °C): δ = 9.50

(br, 2 H^6 of coordinated + uncoordinated Py), 9.00 (br, 1 H^6 of uncoordinated Py), 8.20 (br, 1 H), 8.0 (br, 1 H), 7.50 (br, 3 H), 7.20 (br, 2 H), 7.00 (br, 2 H), 4.10 (brm, 1 H^c), 3.50 (br, 2 H^s), 1.56 (d, J = 9.5 Hz, 2 H^a). – ^{1}H NMR (room temp.): δ = 9.50 (br, 2 H^6), 9.08 (d, J = 4.5 Hz, 1 H^6 of uncoordinated Py), 8.22 (t, J = 7 Hz, 1 H), 8.00 (m, 1 H), 7.58 (m, 1 H), 7.52 (m, 2 H), 7.25 (m, 2 H), 6.94 (d, J = 8 Hz, 2 H), 4.14 (m, 1 H^c), 1.56 (d, J = 9.5 Hz, 2 H^a). – ^{1}H NMR (–60 °C): δ = 9.56 (d, J = 5.5 Hz, 1 H^6 of coordinated Py), 9.11 (d, J = 5.5 Hz, 1 H^6 of uncoordinated Py), 8.98 (d, J = 4 Hz, 1 H^6 of uncoordinated Py), 8.29 (t, J = 8 Hz, 1 H), 8.07 (t, J = 7.5 Hz, 1 H), 7.66 (t, J = 6 Hz, 1 H), 7.57 (q, J = 7 Hz, 2 H), 7.32 (m, 2 H), 7.02 (d, J = 8 Hz, 1 H), 6.85 (d, J = 8 Hz, 1 H), 4.3 (br, 1 H^s), 4.16 (m, 1 H^c), 2.7 (br, 1 H^s), 1.65 (d, J = 9.5 Hz, 1 H^a), 1.50 (d, J = 9.5 Hz, 1 H^a). – IR (CH_2Cl_2): $\tilde{\nu}$ = 1948 vs, 1851s cm^{-1}. – IR (Nujol): $\tilde{\nu}$ = 1940 vs, 1828 vs, 1652 w, 1587 w, 1571 w, 1456 s, 1424 m, 1275 w, 1066 w, 1045 w, 987 w, 807 w, 769 m, 752 w, 737 w cm^{-1}. – $C_{20}H_{17}BrMoN_3O_2P$ (538.19): calcd. C 44.63, H 3.18, N 7.81; found C 44.29, H 3.50, N 7.49. – Conduct. Λ_M ($MeNO_2$): 9 S·cm^2·mol^{-1}.

[Mo(η³-allyl)Br(CO)$_2$(OPPyPh$_2$-*O,N*)] (3): 59%, red. – ^{31}P{^{1}H} NMR (room temp.): δ = 48.6 (br). – ^{31}P{^{1}H} NMR (–60 °C): δ = 51.4 (s, isomer D), 49.5 (s, isomer C). – ^{1}H NMR (room temp.): δ = 9.70 (br, 1 H^6, Py), 7.92 (m, 1 H, Py), 7.73 (m, 9 H, Py + Ph), 7.48 (m, 3 H, Py + Ph), 4.20 (br, 1 H^s), 4.10 (br, 1 H^c), 3.31 (br, 1 H^s), 1.54 (d, J = 9.5 Hz, 1 H^a), 1.31 (d, J = 9.5 Hz, 1 H^a). – ^{1}H NMR (–60 °C): δ = 9.76 (d, J = 5 Hz, 1 H^6, Py, isomer C), 8.98 (d, J = 5 Hz, 1 H^6, Py, isomer D), 7.97 (m, 1 H^6, Py, isomers C + D), 7.76 (m, 9 H, Py + Ph, isomers C + D), 7.48 (m, 3 H, Py + Ph, isomers C + D), 4.35 (br, 1 H^s, isomer C), 4.24 (m, 1 H^c, isomer C), 3.45 (br, 1 H^s, isomer C), 3.38 (br, 1 H^s, isomer D), 3.22 (m, 1 H^c, isomer D), 3.06 (br, 1 H^s, isomer D), 1.55 (d, J = 9.5 Hz, 1 H^a, isomer C), 1.43 (d partially overlapped with the next signal, 1 H^a, isomer D), 1.41 (d, J = 9.5 Hz, 1 H^a, isomer C), 1.27 (d, J = 9.5 Hz, 1 H^a, isomer D); ratio isomer C/isomer D = 1:0.2. – IR (CH_2Cl_2): $\tilde{\nu}$ = 1937 vs, 1838 s cm^{-1}. – IR (KBr pellet): $\tilde{\nu}$ = 3058 w, 1924 vs, 1830 vs, 1588 w, 1485 w, 1459 w, 1439 m, 1314 w, 1285 w, 1167 w, 1152 s, 1141 s, 1123 m, 1086 w, 1073 w, 1055 w, 1027 w, 1012 w, 998 w, 925 w, 766 w, 740 m, 726 m, 695 m, 634 w, 609 w, 560 s, 537 s, 507 w, 481 w, 448 w cm^{-1}. – $C_{22}H_{19}BrMoNO_3P$ (552.22): calcd. C 47.85, H 3.47, N 2.54; found C 47.60, H 3.57, N 2.73. – Conduct. Λ_M ($MeNO_2$): 10 S·cm^2·mol^{-1}.

[Mo(η³-allyl)Br(CO)$_2$(OPPy$_2$Ph-*O,N*)] (4): 72%, orange. Complex **4** was also obtained by an alternative method: A 100 mL Schlenk flask was successively charged with [Mo(CO)$_3$(OPPy$_2$Ph-*O,N*$_2$)] (0.092 g, 0.2 mmol), $CHCl_3$ (20 mL), and allyl bromide (1 mL, 11.5 mmol). An immediate color change from dark purple to orange was observed. After 5 min stirring at room temp., the volatiles were removed in vacuo and the orange residue was recrystallized from CH_2Cl_2/hexane giving 0.052 g (47%) of **4**. – ^{31}P{^{1}H} NMR (room temp.): δ = 39.4 (br, m), 35.4 (s, M). – ^{31}P{^{1}H} NMR (–60 °C): δ = 42.7 (s, isomer D of m), 40.7 (s, isomer C of m), 36.4 (s, isomer D of M), 35.2 (s, isomer C of M). – ^{1}H NMR (room temp.): δ = 9.60 (br, 1 H^6 of coordinated Py, M + m), 8.86 (d, J = 4.5 Hz, 1 H^6 of uncoordinated Py, m), 8.75 (d, J = 4.5 Hz, 1 H^6 of uncoordinated Py, M), 8.39 (t, J = 7 Hz, 1 H, M), 8.24 (m, 1 H, M + m), 7.91 (m, 4H of M + 5 H of m), 7.56 (m, 5 H of M + 5 H of m), 4.20 [br, 1 H^s of (M + m)+ 1 H^c of (M + m)], 3.44 (br, 1H^s of M + m), 1.58 (d, J = 9.5 Hz, 1 H^a of M), 1.56 (d, J = 9.5 Hz, 1 H^a of m), 1.41 (d, J = 9.5 Hz, 1 H^a of m), 1.39 (d, J = 9.5 Hz, 1 H^a of M). – ^{1}H NMR (–60 °C): δ = 9.72 (d, J = 5.5 Hz, 1 H^6 of coordinated Py, isomer C of M), 9.68 (d, J = 5.5 Hz, 1 H^6 of coordinated Py, isomer C of m), 8.90 (brm, 1 H^6 of uncoordinated Py, isomer C + D of m), 8.78 (d, J = 4.5 Hz, 1 H^6 of uncoordinated Py, isomer C of M), 8.72 (d, J = 4.5 Hz, 1 H^6 of uncoordinated Py, isomer D of M), 8.33 (m), 7.96 (m), 7.62 (m), 4.39 (br, 1 H^s, isomer C of M + m), 4.30 (m, 1 H^c, isomer C of M + m), 3.61 (br, 1 H^s, isomer C of m), 3.52 [br, 1 H^s of isomer C of m and 1 H^c of isomer D (M or m)], 3.25 [m, 1 H^c of isomer D (M or m)], 3.18 (br, 1 H^s, isomer D of M), 3.16 (br, 1 H^s, isomer D of m), 1.61 (d, J = 9.5 Hz, 1 H^a, isomer C of M), 1.58 (d, J = 9.5 Hz, 1 H^a, isomer C of m), 1.50 (d, J = 9.5 Hz, 1 H^a, isomer C of m), 1.43 (d, J = 9.5 Hz, 1 H^a, isomer C of M), 1.35 (m, H^a, isomer D of M + m); M = major equilibrium; m = minor equilibrium; ratio M/m = 1:0.8; Ratio isomer C/isomer D for each equilibrium = 1:0.2. –

Table 2. Crystal data and structure refinement for **5**

Empirical formula	$C_{20}H_{17}BrMoN_3O_3P$
Formula weight	554.17
Temperature	293(2) K
Wavelength	0.71073 Å
Crystal system	Monoclinic
Space group	C2/c
Unit cell dimensions	a = 20.5279(14) Å, α = 90°
	b = 12.0329(8) Å, β = 96.146(10)°
	c = 17.1172(11) Å, γ = 90°
Volume	4203.8(5) Å^3
z	8
Density (calculated)	1.751 Mg/m^3
Absorption coefficient	2.627 mm^{-1}
F(000)	2192
Crystal size	0.2 × 0.2 × 0.15 mm
Theta range for data collection	2.24 to 25.02°
Index ranges	–17 h 24, –14 k 14, –19 l 20
Reflections collected	9749
Independent reflections	3685 [R(int) = 0.0534]
Refinement method	Full-matrix least-squares on F^2
Data/restraints/parameters	3679/0/262
Goodness-of-fit on F^2	1.154
Final R indices [$I > 2\sigma(I)$]	$R1$ = 0.0485, $wR2$ = 0.0897
R indices (all data)	$R1$ = 0.0830, $wR2$ = 0.1078
Weighting scheme calc.	$1/[\sigma^2(F_o^2) + (0.0297\ P)^2 + 16.4861\ P]$, where $P = (F_o^2 + 2\ F_c^2)/3$
Largest diff. peak and hole	0.0384 and –0.494 e/Å^3

IR (CH_2Cl_2): $\tilde{\nu}$ = 1950 s(sh), 1937vs, 1858 m(sh), 1839 s cm^{-1}. – IR (KBr pellet): $\tilde{\nu}$ = 3060 w, 1923 vs, 1828 vs, 1587 w, 1574 w, 1440 m, 1285 w, 1169 m, 1154 m, 1134 s, 1096 m, 1011 w, 988 w, 807 w, 774 w, 748 s, 694 w, 560 s, 540 s, 508 w, 449 w cm^{-1}. – $C_{21}H_{18}BrMoN_2O_3P$ (553.21): calcd. C 45.59, H 3.28, N 5.06; found C 45.36, H 3.01, N 5.06. – Conduct. Λ_M ($MeNO_2$): 18 $S{\cdot}cm^2{\cdot}mol^{-1}$.

[Mo(η^3-allyl)Br(CO)$_2$(OPPy$_3$-*O*,*N*)] (5): 47%, red. – $^{31}P\{^1H\}$ NMR (room temp.): δ = 34.0 (br). – $^{31}P\{^1H\}$ NMR (–60 °C): δ = 36.4 (s, isomer C), 32.1 (s, isomer D). – ^1H NMR (room temp.): δ = 9.50 (br, 1 H^6 of coordinated Py), 8.82 (d, J = 4.5 Hz, 1 H^6 of uncoordinated Py), 8.70 (d, J = 4.5 Hz, 1 H^6 of uncoordinated Py), 8.37 (m, 2 H), 7.90 (m, 4 H), 7.69 (br, 1 H), 7.51 (m, 1 H), 7.44 (m, 1 H), 4.10 (br, 1 H^s + 1 H^c), 3.40 (br, 1 H^s), 1.54 (d, J = 9.5 Hz, 1 H^a), 1.36 (d, J = 9.5 Hz, 1 H^a). – ^1H NMR (–60 °C): δ = 9.76 (d, J = 5 Hz, 1 H^6 of coordinated Py, isomer C), 8.94 (d, J = 5 Hz, 1 H^6 of coordinated Py, isomer D), 8.88 (d, J = 4.5 Hz, 1 H^6 of uncoordinated Py, isomer C), 8.84 (d, J = 4.5 Hz, 1 H^6 of uncoordinated Py, isomer D), 8.76 (d, J = 4.5 Hz, 1 H^6 of uncoordinated Py, isomer C), 8.72 (d, J = 4.5 Hz, 1 H^6 of uncoordinated Py, isomer D), 8.50 (t, J = 7 Hz, 1 H, isomer D), 8.43 (t, J = 6.5 Hz, 1 H, isomer C), 8.27 (t, J = 7 Hz, 1 H, isomer C), 8.22 (t, J = 6.5 Hz, 1 H, isomer D), 7.90 (m, 5 H, isomers C + D), 7.60 (m, 1 H, isomers C + D), 7.50 (d, J = 5 Hz, 1 H, isomers C + D), 4.37 (br, 1 H^s, isomer C), 4.27 (m, 1 H^c, isomer C), 3.82 (m, 1 H^c, isomer D), 3.55 (br, 1 H^s, isomer C), 3.33 (br, 1 H^s, isomer D), 3.26 (br, 1 H^s, isomer D), 1.59 (d, J = 9.5 Hz, 1 H^a, isomer C), 1.47 (d, J = 9.5 Hz, 1 H^a, isomer D), 1.41 (d, J = 9.5 Hz, 1 H^a, isomer C), 1.38 (d, J = 9.5 Hz, 1 H^a, isomer D); ratio isomer C/isomer D = 1:0.9. – IR (CH_2Cl_2): $\tilde{\nu}$ = 1950 vs, 1854 s cm^{-1}. – IR (Nujol): $\tilde{\nu}$ = 1936 vs, 1838 vs, 1589 w, 1577 m, 1430 m, 1285 w, 1220 w, 1177 m, 1163 m, 1148 m, 1104 m, 1085 m, 1057 w, 1010 w, 988 w, 771 w, 748 m cm^{-1}. – $C_{20}H_{17}BrMoN_3O_3P$ (554.19): calcd. C 43.35, H 3.09, N 7.58; found C 43.27, H 3.17, N 7.69. – Conduct. Λ_M ($MeNO_2$): 20 $S{\cdot}cm^2{\cdot}mol^{-1}$.

X-ray Crystallographic Analysis of 5: Crystal data and other details of the structure analysis are presented in Table 2. Red crystals of **5** were recrystallized from dichloromethane/diethyl ether and showed a block-like habit. One of these crystals was mounted on a glass fiber with epoxy resin. All diffraction measurements were made at room temperature with a Siemens SMART[25] diffractometer using graphite monochromated Mo-K_α radiation. A full hemisphere of reciprocal space was scanned by 0.3° ω steps with the area detector center held at 2θ = –27°. A total of 1321 data frames were collected for 10 seconds exposure per frame. The reflections were integrated using the SAINT program.[26] No crystal decay over the period of data collection was observed. A total of 10001 diffracted intensities were measured, 3685 unique observations remained after averaging of duplicate and equivalent measurements (R_{int} = 0.0579) and deletion of the systematic absences. Of these 2587 had $I > 2\sigma(I)$. An empirical absorption and detector correction was applied, effective transmission coefficients were in the range 0.878 to 0.634. Lorentz and polarization corrections were applied. The structure was solved by direct and Fourier methods, and refined using full-matrix least-squares refinement on F^2.[27] All non-hydrogen atoms were assigned anisotropic displacement parameters and refined without positional constraints. All hydrogen atoms were constrained to idealized geometries and assigned isotropic displacement parameters 1.2 times the U_{iso} value of their attached carbon for aromatic hydrogens. Final residuals and other details are given in Table 1.[28] Weights, w, were set to minimize the variation in S as a function of $|F_o|$. Final difference electron density maps showed no significant features. Complex neutral-atom scattering factors were taken from ref.[29].

Crystallographic data (excluding structure factors) for the structure reported in this paper have been deposited with the Cambridge Crystallographic Data Centre as supplementary publication no. CCDC-134122. Copies of the data can be obtained free of charge on application to CCDC, 12 Union Road, Cambridge CB2 1EZ, UK [Fax: (internat.) + 44-1223/336-033; E-mail: deposit@ccdc.cam.ac.uk].

Acknowledgments

The authors in Valladolid thank the D.G.I.C.Y.T. of Spain for financial support (Project PB96–0363), and the Bristol authors the UK EPSRC for financial support.

[1] [1a] J. A. Casares, S. Coco, P. Espinet, Y.-S. Lin, *Organometallics* **1995**, *14*, 3058–3067. – [1b] J. A. Casares, P. Espinet, J. M. Martínez-Ilarduya, Y.-S. Lin, *Organometallics* **1997**, *16*, 770–779. – [1c] J. A. Casares, P. Espinet, *Inorg. Chem.* **1997**, *36*, 5428–5431.

[2] [2a] P. Espinet, P. Gómez-Elipe, F. Villafañe, *J. Organomet. Chem.* **1993**, *450*, 145–150. – [2b] J. A. Casares, P. Espinet, R. Hernando, G. Iturbe, F. Villafañe, D. D. Ellis, A. G. Orpen, *Inorg. Chem.* **1997**, *36*, 44–49.

[3] G. R. Newkome, *Chem. Rev.* **1993**, *93*, 2067–2089.

[4] M. D. Curtis, O. Eisenstein, *Organometallics* **1984**, 3, 887–895.

[5] [5a] R. Davis, L. A. P. Kane-Maguire, in *Comprehensive Organometallic Chemistry* (Eds.: G. Wilkinson, F. G. A. Stone, E. W. Abel), Pergamon, Oxford, UK, **1982**, Volume 8, 1156–1159. – [5b] M. W. Whiteley, in *Comprehensive Organometallic Chemistry II* (Eds.: G. Wilkinson, F. G. A. Stone, E. W. Abel), Pergamon, Oxford, UK, 1995. Volume 12, J. A. Labinger, M. J. Winter, eds.; 337–338.

[6] M. P. T. Sjögren, H. Frisell, B. Åkermark, P.-O. Norrby, L. Eriksson, A. Vitagliano, *Organometallics* **1997**, *16*, 942–950.

[7] F. A. Cotton, R. L. Luck, *Acta Crystallogr., Sect. C* **1990**, *46*, 138–140.

[8] J. W. Faller, D. A. Haitko, R. D. Adams, D. F. Chodosh, *J. Am. Chem. Soc.* **1979**, *101*, 865–876.

[9] I. Ugi, D. Marquarding, H. Klusacek, P. Gillespie, *Acc. Chem. Res.* **1971**, *4*, 288–296.

[10] [10a] B. J. Brisdon, M. Cartwright, A. G. W. Hodson, M. F. Mahon, K. C. Molloy, *J. Organomet. Chem.* **1992**, *435*, 319–335. – [10b] B. J. Brisdon, M. Cartwright, A. G. W. Hodson, *J. Organomet. Chem.* **1984**, *277*, 85–90. – [10c] K.-B. Shiu, K.-S. Liou, C. P. Cheng, B.-R. Fang, Y. Wang, G.-H. Lee, W.-J. Vong, *Organometallics* **1989**, *8*, 1219–1224.

[11] K.-B. Shiu, C.-J. Chang, S.-L. Wang, F.-L. Liao, *J. Organomet. Chem.* **1991**, *407*, 225235.

[12] [12a] S. K. Chowdhury, M. Nandi, V. S. Joshi, A. Sarker, *Organometallics* **1997**, *16*, 1806–1809. – [12b] D. S. Frohnapfel, P. S. White, J. L. Templeton, H. Rüegger, P. S. Pregosin, *Ibid* **1997**, *16*, 3737–3750. – [12c] K.-B. Shiu, C.-J. Chang, Y. Wang, M.-C. Cheng, *J. Organomet. Chem.* **1991**, *406*, 363–369.

[13] The preparation of **1** was described previously in ref.[2a], but the structure was assigned mistakenly from the 80 MHz NMR data. The new data now available from a 300 MHz apparatus allows us to correct that mistake here.

[14] R. P. Schutte, S. J. Rettig, A. M. Joshi, B. R. James, *Inorg. Chem.* **1997**, *36*, 5809–5817.

[15] [15a] P. K. Byers, A. J. Canty, *Organometallics*, **1990**, *9*, 210–220. – [15b] R. E. Rülke, J. M. Ernsting, A. L. Spek, C. J. Elsevier, P. W. N. M. Leeuwen, K. Vrieze, *Inorg. Chem.* **1993**, *32*, 5769–5778.

[16] $(CD_3)_2CO$ solution has to be used in order to avoid ion pairs detected in $CDCl_3$ solutions (ref.[1a]).

[17] K. Nakamoto, *Infrared and Raman Spectra of Inorganic and Coordination Compounds*, 3rd ed., Wiley, New York, **1978**, p. 209.

[18] B. J. Brisdon, A. A. Woolf, *J. Chem. Soc., Dalton Trans.* **1978**, 291–295.

[19] M. A. Alonso, J. A. Casares, P. Espinet, K. Soulantica, *Angew. Chem. Int. Ed. Eng.* **1999**, *38*, 533–535.

[20] D. D. Perrin, W. L. F. Armarego, *Purification of Laboratory Chemicals*, 3rd ed., Pergamon Press, Oxford, **1988**.

[21] H. tom Dieck, H. Friedel, *J. Organomet. Chem.* **1968**, *4*, 375–385.
[22] [22a] F. R. Keene, M. R. Snow, P. J. Stephenson, E. R. T. Tiekink, *Inorg. Chem.* **1988**, *27*, 2040–2045. – [22b] K. Kurtev, D. Ribola, R. A. Jones, D. J. Cole-Hamilton, G. Wilkinson, *J. Chem. Soc., Dalton Trans.* **1980**, 55–58. – [22c] H. Schmidbaur, Y. Inoguchi, *Z. Naturforsch, Teil B.* **1980**, *35*, 1329–1334.
[23] [23a] F. G. Mann, J. Watson, *J. Org. Chem.* **1948**, *13*, 502–531. – [23b] G. R. Newkome, D. C. Hager, *J. Org. Chem.* **1978**, *43*, 947–949.
[24] W. Geary, *Coord. Chem. Rev.* **1971**, *7*, 81–122.
[25] SMART Siemens Molecular Analysis Research Tool V4.014 copyright **1989–94**, Siemens Analytical X-ray, Madison, WI, USA.
[26] SAINT (Siemens Area detector INTegration) program, Siemens Analytical X-ray, Madison, WI, USA.
[27] SHELXTL Rev. 5.0, Siemens Analytical X-ray, 1994.
[28] $R1 = \Sigma||F_o| - |F_c||/\Sigma|F_o|$; $wR2 = [\Sigma w(F_o^2 - F_c^2)^2/\Sigma w(F_o^2)^2]^{1/2}$; $S = [\Sigma w(F_o^2 - F_c^2)^2/(N - NV)]^{1/2}$; ($N$ = data + restraints; NV = parameters).
[29] *International Tables for Crystallography*, Vol. C, **1992**, Kluwer, Dordrecht.

Received October 14, 1999
[I99363]